Construction and Building Materials 438 (2024) 137195

Contents lists available at ScienceDirect

Construction and Building Materials

journal homepage: www.elsevier.com/locate/conbuildmat

Acoustic behaviour of GFRP-PUR web-core composite sandwich panels

Miguel Proença [a,1], Pedro Santos [b], Luís Godinho [b], Albano Neves e Sousa [a], João R. Correia [a,*], Mário Garrido [a], José Sena-Cruz [c]

[a] CERIS, Instituto Superior Técnico, Universidade de Lisboa, Portugal
[b] University of Coimbra, ISISE, ARISE, Department of Civil Engineering, Coimbra, Portugal
[c] University of Minho, ISISE, ARISE, Campus de Azurém, Guimarães, Portugal

ARTICLE INFO

Keywords:
Sandwich panels
Glass fibre reinforced polymer
Polyurethane foam core
Airborne sound reduction
Impact sound pressure level

ABSTRACT

This paper presents an experimental and analytical study about the sound insulation of innovative sandwich panels - named *EasyFloor* – for the rehabilitation of degraded timber floors in old buildings. Two types of panels were developed: (i) an all-composite sandwich panel, made of glass fibre reinforced polymer (GFRP) face sheets and webs, and polyurethane (PUR) foam; (ii) and a hybrid sandwich panel, where the top face sheet comprises a thin layer of concrete. The study included the comparative analysis of the airborne sound reduction and impact sound pressure level of both types of panels based on experimental tests on full-scale specimens, including a typical floor covering. The acoustic insulation properties determined experimentally were compared with predictions from different analytical models typically applied to sandwich panels, and also with performance requirements defined in building regulation. Among the different analytical models that were assessed, Sharp's model provided the most accurate predictions when considering the natural and dilatation frequencies as the critical frequency. The comparison of the normalized airborne and impact sound indices determined experimentally with requirements set in building regulation shows that the use of GFRP-PUR panels in the rehabilitation of lightweight timber floors and in new construction, where building comfort requirements are stricter, require mitigation measures to improve sound insulation.

1. Introduction

Sandwich panels are composite-section building components that typically comprise thin face sheets bonded to a low-density core [1–3]. Such type of panels is widely used in civil engineering applications mainly as non-structural or secondary components subjected to low load levels, such as cladding or roof sheeting. However, their application as primary structural members has also been investigated, namely in bridge [4–6] and pier decks [7], and in building floors [8], for both new construction and rehabilitation. In contrast to the more typical lightweight configuration, for some heavier applications, sandwich solutions can comprise relatively thick steel sheets and high-density elastomeric cores [9].

Regarding the constituent materials of sandwich panels, alternatives to typical metal sheets include fibre-reinforced polymer (FRP) composites [10–13], such as glass fibre-reinforced polymer (GFRP), which are often combined with lightweight cores, such as polyurethane (PUR) foam [14,15]. Advantages offered by FRP composites when compared to metallic-based solutions include their lower self-weight, high strength-to-weight ratio, improved durability and reduced maintenance requirements [16,17]. The prefabrication possibilities (*e.g.*, vacuum infusion or pultrusion) and low self-weight of FRP composites renders such composite sandwich panels an interesting solution for old building floors, namely in rehabilitation scenarios, where the existing structural members (often stone-rubble masonry walls) are usually not able to withstand significant weight increase; rehabilitation solutions with FRP sandwich panels involve lower overall vertical loads than traditional solutions (*e.g.*, reinforced concrete slabs), which avoids affecting the original seismic performance of such buildings [14].

Despite such advantages, and as a result of their low weight, a weak point in such type of elements is the poor acoustic performance for both airborne and impact sound transmission [18] compared to conventional solutions, which means that additional sound transmission mitigation measures (such as false ceilings and/or floorings supported on a resilient

* Corresponding author.
E-mail address: joao.ramoa.correia@tecnico.ulisboa.pt (J.R. Correia).
[1] † deceased

https://doi.org/10.1016/j.conbuildmat.2024.137195
Received 11 January 2024; Received in revised form 20 June 2024; Accepted 21 June 2024
Available online 1 July 2024

layer) should be needed to fulfill user comfort requirements for housing and office buildings. The recent work by Proença *et al.* [14] on the acoustic performance (for airborne and impact sounds) of homogeneous-core GFRP-PUR sandwich panels for structural applications highlights such need for additional detailing of corrective measures to comply with building code requirements.

In the follow-up of the development and study of homogeneous core GFRP-PUR sandwich panels [14], a novel web-core composite sandwich panel design was proposed as a modular system, named *EasyFloor*. Two variants of this *EasyFloor* sandwich system were developed for building floors: (i) an all-composite sandwich panel, made of GFRP face sheets and webs, and PUR infill foam (Fig. 1a), for spans up to 4 m; (ii) and a hybrid sandwich panel, where the top face sheet is made of a thin layer of concrete (Fig. 1b), for spans up to 5 m. Adjacent panels can be connected vertically through a snap-fit or horizontally by means of adhesive bonding (without snap-fit).

The present paper aims at assessing the acoustic performance of such web-core sandwich panel systems, through the accomplishment of the following goals: analysis of their (i) airborne sound reduction and (ii) impact sound pressure level based on experimental tests on full-scale specimens; (iii) experimental assessment of the impact sound reduction provided by a typical floor covering; (iv) comparison of the acoustic insulation properties determined experimentally with corresponding analytical predictions; and (v) verification of the compliance with building code requirements for the acoustic insulation properties of the sandwich panels.

The remainder of the paper is organized as follows: (i) a literature review is presented first, summarizing the main findings from previous studies more directly related with this study; next, (ii) the materials and test methods are described, and (iii) the experimental results are presented and (iv) compared with analytical predictions; (v) the compliance with the design requirements and typical building regulations is assessed; and, finally, (vi) the main conclusions drawn from this study are presented.

2. Literature review

In general, wave motion in a sandwich panel subjected to an acoustical excitation may be separated into four basic motions: (i) symmetric motion (often related to longitudinal waves); (ii) anti-symmetric motion (relative to flexural/bending waves); (iii) dilatational motion (propagation of a wave through the thickness); and (iv) shear waves. D'Alessandro *et al.* [18] presented an extensive review of theoretical and numerical models for the acoustic analysis of sandwich panels, including methods such as the Finite Element Method (FEM), the Boundary Element Method (BEM) or Statistical Energy Analysis (SEA). Besides these advanced models, simpler analytical/empirical models for sandwich-type panels were proposed by different authors, such as Krakers [19] and Ballagh [20].

Few studies are available in the literature about the acoustic behaviour of sandwich panels similar to the one developed herein for building applications. Patinha *et al.* [21] performed tests to characterize the sound insulation properties of hybrid composite sandwich specimens made of jute and glass fibre hybrid face sheets with three different fibre architectures and extruded PUR cores. However, the test setup adopted was quite unique, precluding the comparison of results with experimental data for other sandwich solutions, and pointing out the need for test results obtained via standardized testing procedures. Garay and Pino [22] performed laboratory measurements for the determination of the airborne sound reduction index (R_w) of a sandwich panel made of expanded polystyrene (EPS) core and oriented-strand board (OSB) face sheets, and obtained a R_w value of 39 dB. Petrone *et al.* [23] studied the acoustic power radiated from sandwich panels made of aluminum foam via experimental testing and numerical modelling, and concluded that the models adopted were able to predict the experimental results when assuming a constant damping factor. Wawrzynowicz *et al.* [24] performed experimental tests and analytical and numerical (including finite element) simulations to determine the airborne sound insulation of a composite sandwich panel made of magnesium-cement face sheets and EPS core. FE models compared well with test results, while the analytical model provided accurate predictions until 1600 Hz. Santos *et al.* [25] performed airborne and impact sound transmission tests on a sandwich panel made of cross-ply wood layers and a PUR foam core on a reduced-size chamber based on test protocols from ISO 10140–2 [26] and ISO 10140–3 [27]. They found out that analytical models developed to describe the airborne sound insulation of typical sandwich panels (*i. e.*, with thin and rigid face sheets and thick soft core) were able to simulate the experimental behaviour of a metal-sheet sandwich panel, but failed to describe the behaviour of the panels they had developed, which comprised thicker face sheets. From a series of tests on different analytical models, they found out that the Sharp model for homogeneous isotropic elements [28] with an adaptation (the replacement of the typical critical frequency due to bending by the dilatational frequency) provided the best fit to test results. Proença *et al.* [14] performed standard airborne and impact sound transmission tests on full-scale homogeneous-core composite sandwich panels made of GFRP face sheets and PUR core, designed for residential building floors; the study included also numerical and analytical simulations for the assessment of airborne and impact sound insulations, respectively. The numerical and analytical simulations presented good agreement with the experimental data. Furthermore, results revealed an overall poor acoustic performance of those panels, pointing out the need for additional non-structural elements to fulfill the acoustic requirements set in building codes, for both airborne and impact sounds. Such need was also reported in the experimental study by Nurzynski and Nowotny [15], which assessed different strategies (plasterboard suspended ceilings, different types of floor coverings and floating screeds) to improve the acoustic performance of composite panels for both types of sounds. However, the study focused on non-structural composite panels (total thickness of 35 mm and 60 mm, with very low surface mass, 10–12 kg/m^2); the experiments presented in this study were not complemented with any analytical or numerical simulations.

The *EasyFloor* composite sandwich panels present some similarities with previous solutions, namely with the homogeneous-core panel studied by Proença *et al.* [14]. However, the *EasyFloor* sandwich panels also comprise relevant differences, namely: (i) its web-core shape of the cross-section; and (ii) the use of a concrete top face sheet in the hybrid variant. These intrinsic differences and the envisaged application justify

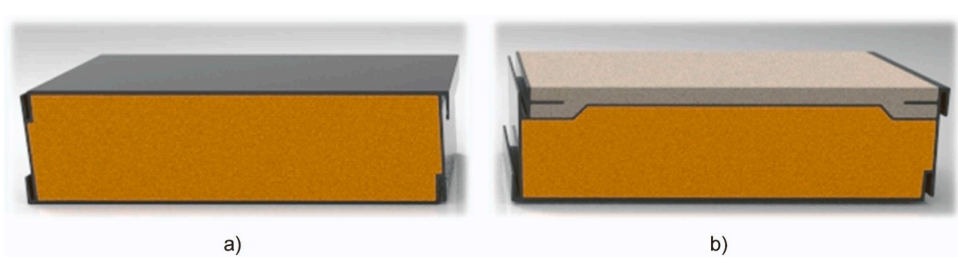

Fig. 1. *EasyFloor* sandwich panel variants comprising the snap-fit connection: a) all-composite and b) hybrid.

the need to investigate the acoustic behaviour of this novel type of panels, by means of experimental tests, as well as to assess the validity of analytical models available in the literature to describe such behaviour.

3. Materials and test methods

3.1. Materials and specimen's preparation

For both all-composite and hybrid sandwich panels, two different types of geometries were considered for the test specimens: (i) panels with plan dimensions of 1.508 × 1.250 m^2 for the airborne sound reduction tests (Fig. 2); and (ii) panels with plan dimensions of 1.508 × 1.600 m^2 for the impact sound pressure level tests (Fig. 3).

The specimens were composed of five segments of the *EasyFloor* panel, each with 0.30 m of width and length dependent on the type of test (1.25 m for the airborne sound tests and 1.60 m for the impact sound tests), adhesively bonded together along the side edges (this connection had an average adhesive thickness of 2 mm). The reference all-GFRP sandwich panel was composed of a PUR core with density of 70 kg/m^3 and GFRP face sheets and webs with thicknesses of 5.5 mm and 7.7 mm, respectively (average tensile modulus in the longitudinal direction of 31.4 GPa and 26.0 GPa, respectively). The GFRP-concrete hybrid sandwich panel had an additional 20 mm thick layer of C30/37 concrete placed over the top GFRP face sheet (average cylinder compressive strength of 42.3 MPa, average flexural tensile strength of 5.5 MPa). The all-GFRP and the hybrid sandwich panels mass per unit area was 41.7 kg/m^2 and 89.7 kg/m^2, respectively.

A two-component thixotropic epoxy adhesive (*Sikadur®–31 EF*) produced by *Sika* was adopted to perform the panel-to-panel connection. The epoxy adhesive was applied to the all-GFRP specimens and cured in laboratory conditions (temperature and relative humidity). For this purpose, the side surfaces (lateral edges) of the panels were firstly sanded with sandpaper, to increase the roughness of the surface, and then cleaned with acetone to remove any oils or debris, prior to the application of the adhesive. A base plate made of plywood was prepared with a plastic film on top of it (Fig. 4a), to prevent the adhesive from adhering to the base plate. Then, the two-component adhesive was mixed and applied to the side surfaces of the panel segments (Fig. 4b), and these were placed side-by-side on top of the base plate (Fig. 4c). After placing and carefully aligning all five segments of composite sandwich panels, two straps were placed transversely to the segments, along the web of an I-shaped GFRP profile, and firmly tightened (Fig. 4d). Finally, the excess of squeezed adhesive was removed.

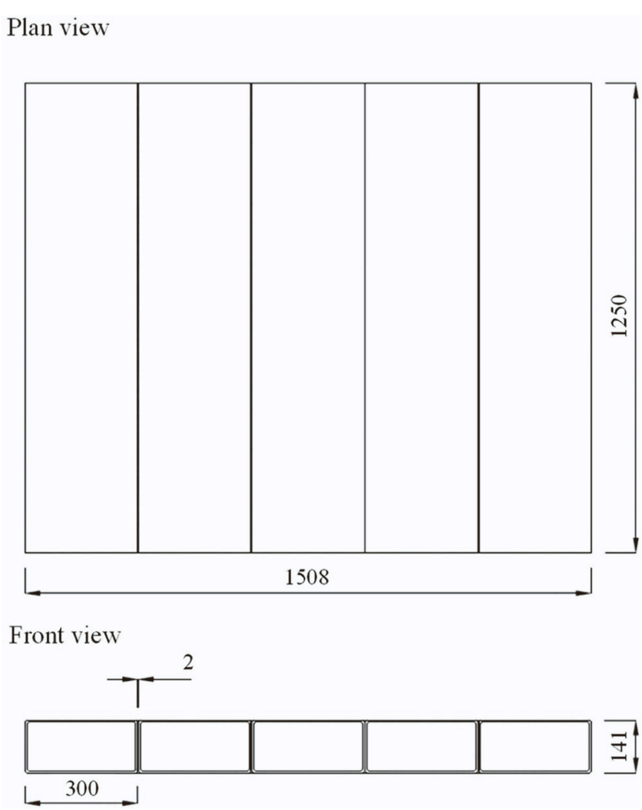

Fig. 2. Airborne sound reduction test specimen geometry – homogeneous-core sandwich panel (in mm).

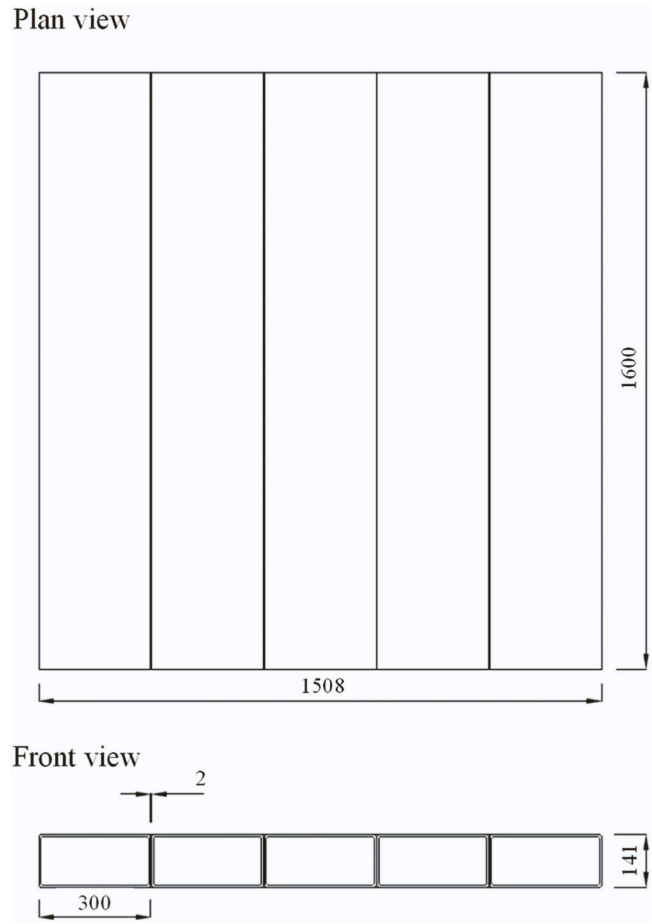

Fig. 3. Impact sound pressure level test specimen geometry – homogeneous-core sandwich panel (in mm).

The hybrid panel specimens were produced following the same adhesive application methodology. After the 5-day cure of the adhesive, the specimens were prepared for concreting. Similarly to the bonded lateral faces, the top surface of the panels was firstly sanded with sandpaper, to increase the roughness of the surface, and then cleaned with acetone to remove any oils or debris. Then, a formwork was prepared with wooden boards around each panel, fixed by two threaded rods on each side (Fig. 5a). The *Sikadur®–32 EF* adhesive, produced by *Sika*, was applied on the (GFRP) top face sheet of the panel (Fig. 5b) to improve the bond between the GFRP and fresh (wet) concrete. Afterwards, the concrete was poured onto the mould (Fig. 5c). Lastly, the concrete was screeded with a flat board to achieve a smooth and flat finish (Fig. 5d).

3.2. Airborne sound insulation tests

The airborne sound insulation tests were performed according to ISO 10140–2 [26]. The standard requires the use of two large-scale adjacent reverberation rooms, with a test specimen of about 10 m^2 plan area

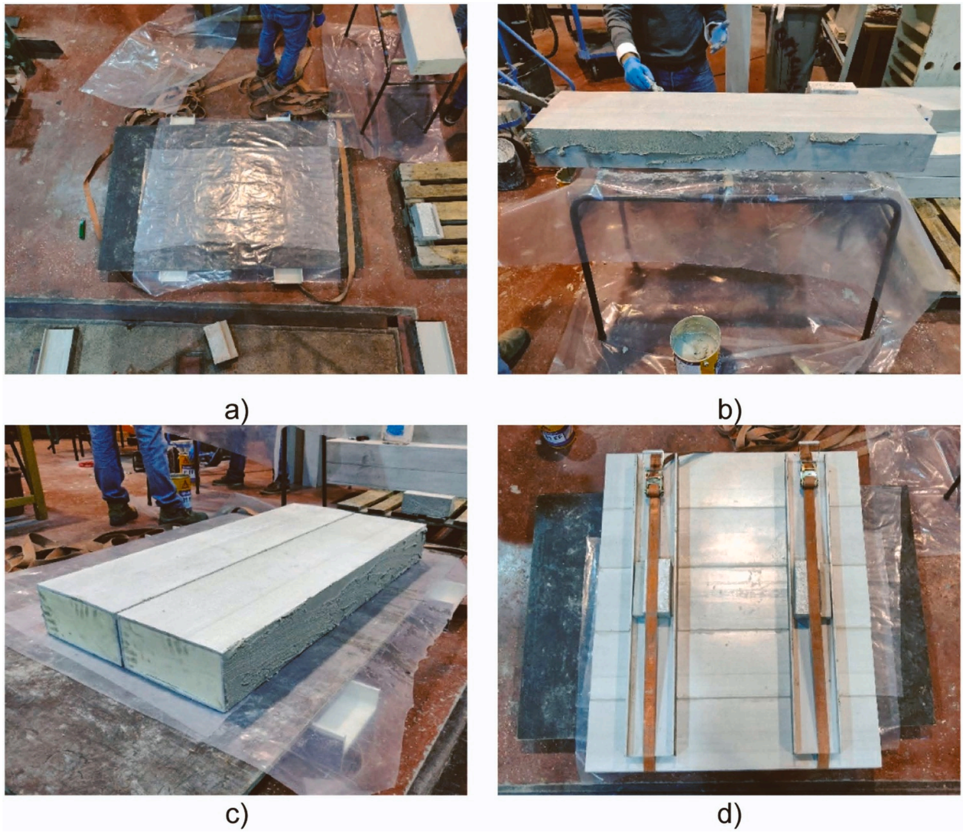

Fig. 4. Preparation of the acoustic test specimens: a) base plate; b) application of the adhesive on the edge of one panel segment; c) placement of the panel segments side-by-side; d) tightening of the straps around the five panel segments.

placed in between the two rooms. The chambers where the tests were performed consist of two contiguous rooms, the source and receiving chambers, with internal volumes of 111 m^3 and 122 m^3, respectively; these rooms are separated by a high sound insulation wall with an opening where the test specimen was placed.

As for the size of the test specimen, in this work, a smaller sized panel (1.5 m x 1.3 m) has been used, due to production and equipment limitations. Indeed, the standard also accounts for this possibility, although some care should be taken in the interpretation of the results in such cases, particularly when the wavelength of the bending wave is higher than half of the minimum size of the panel (0.625 m in the present case). The bending wavelength of an orthotropic sandwich panel (λ_b) depends on the wave direction and equals that of the isotropic equivalent plate for the case of a flexural wave propagating in the principal directions. For other directions, it is affected by the shear constant [29]. Fig. 6 illustrates the bending wavelength as a function of the direction and frequency, for the all-GFRP (Fig. 6a) and hybrid panels (Fig. 6b). It can be seen that below 1900 Hz in the all-GFRP panel, and 2500 Hz in the hybrid panel, the smaller dimensions of the panel may influence the sound reduction results.

The modal behaviour of the tested specimens has also been analysed, and the lower order natural frequencies are shown in Table 1, considering an equivalent plate approach and simply supported edges. Table 1 confirms that only few vibration modes are estimated to occur in this frequency region in the all-GFRP and hybrid sandwich panels, considering an equivalent plate approach, as given in Eq. (1),

$$R\omega_{n_x n_y} = \frac{\pi^2}{\sqrt{m}}\sqrt{\frac{n_x^4}{b_x^4}B_x + \frac{n_x^2}{b_x^2}\bullet\frac{n_y^2}{b_y^2}B_{xy} + \frac{n_y^4}{b_y^4}B_y} \tag{1}$$

where $\omega_{n_x n_y}$ are the natural frequencies obtained, for modes $(n_x n_y)$, for a simply supported orthotropic plate with an equivalent thickness h; and B_x, B_y and B_{xy} correspond, respectively, to the flexural bending stiffness along the principal directions and the transverse shear stiffness. It can be seen that only few vibration modes are estimated to occur below 2000 Hz, both in the all-GFRP and hybrid sandwich panels. These results indicate that the experimental measurements may be affected by the modal behaviour exhibited by the panels at lower frequencies.

The following equipment was used for the tests: (i) a data acquisition device, *Symphonie 01 dB*; (ii) two ½" microphones, *GRAS* model *46 A*; and (iii) a sound source *Brüel & Kjær*, model *OMNIPOWER 4292*. The acquisition and processing of the signal was performed using *dBBATI32* software that converts the sound pressure level directly into the frequency domain.

The positions of the microphones (labelled 1–5) and the sound sources (labelled F1 and F2) in the acoustic source chamber are shown in Fig. 7 and the five adopted positions of the microphones for the receiving chamber (labelled 1–5) are presented in Fig. 8. These microphones were located at least 0.8 m apart from the wall to mitigate close-to-wall effects, following normative references of ISO 10140–4 [30].

Measurements were performed considering two repetitions for each combination of: (i) source position; (ii) microphone position in the source room, and (iii) microphone position in the receiving room. This involved a total of 100 measurements for each airborne sound pressure test.

Fig. 9 shows the receiving and source rooms with the all-GFRP and hybrid sandwich panels placed on the test opening. Regarding the hybrid sandwich panel, the specimen was placed with the concrete layer facing the source room. After placing the specimens inside the opening, compressed mineral wool was introduced around the specimens to mitigate any gaps. Furthermore, a thin line of silicone was applied to both sides of the contour of the specimens, and left to cure for 24 hours. The panels can be considered to be simply supported along all edges, as small displacements and rotations were possible within the compressed

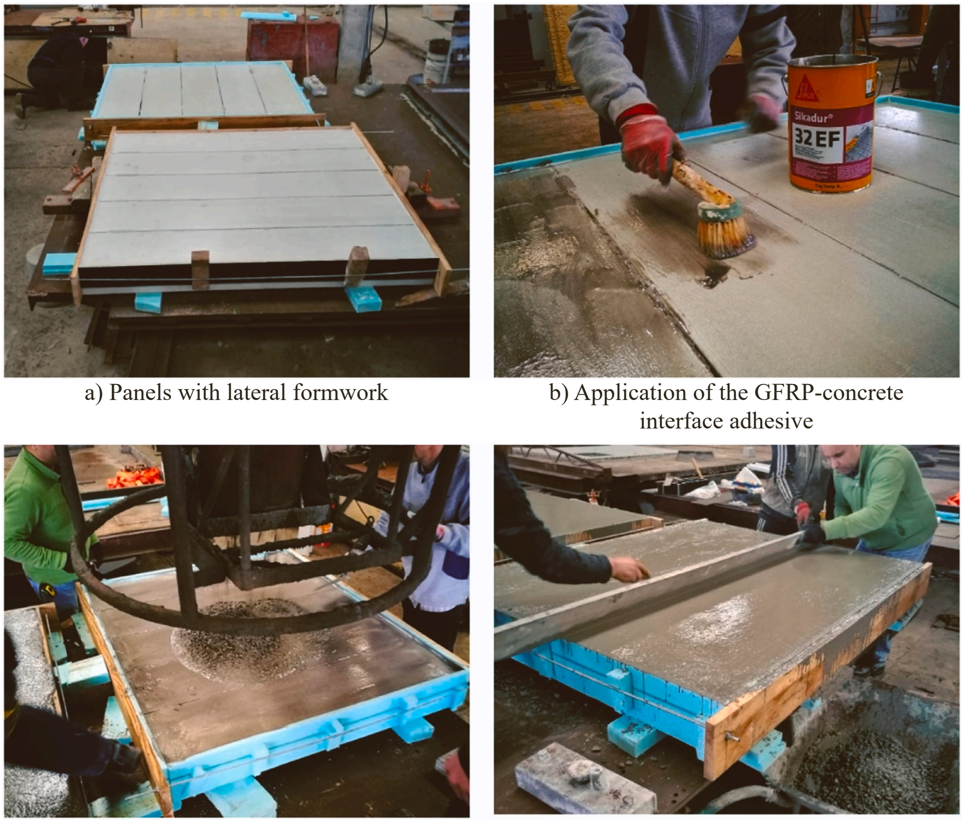

a) Panels with lateral formwork
b) Application of the GFRP-concrete interface adhesive
c) Pouring of the concrete
d) Screeding of the concrete

Fig. 5. Preparation of the hybrid sandwich panel.

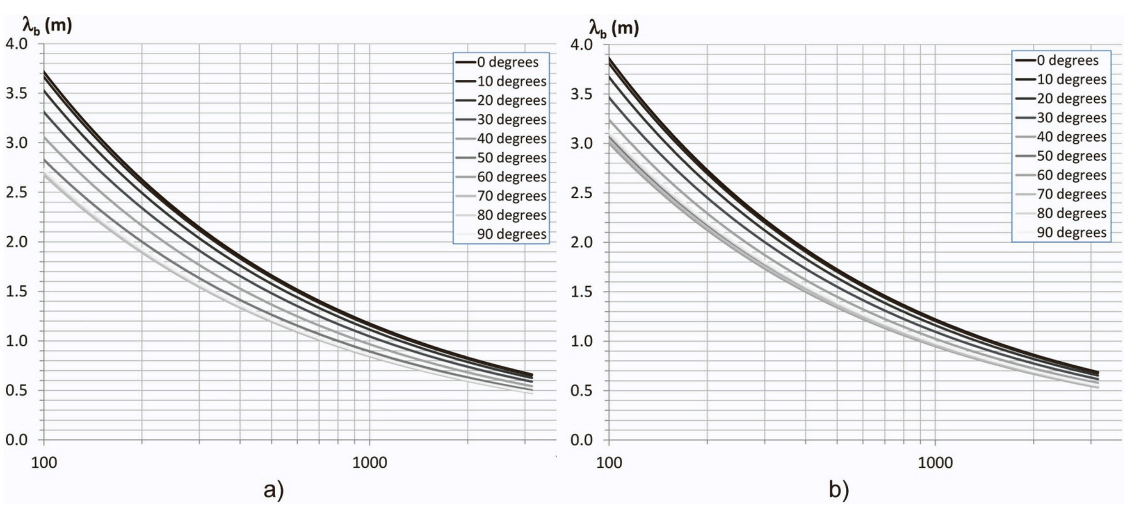

Fig. 6. Bending wavelength spectra for different angles of the wave with the longitudinal direction: a) all-GFRP sandwich panel; b) hybrid sandwich panel.

Table 1
Estimated natural frequencies for the all-GFRP and hybrid sandwich panels.

Panel	Natural frequencies (Hz)									
All-GFRP	$f_{1,1}$	$f_{1,2}$	$f_{1,3}$	$f_{2,1}$	$f_{2,2}$	$f_{2,3}$	$f_{1,4}$	$f_{2,4}$	$f_{3,1}$	$f_{3,2}$
	254.1	438.9	821.5	907.7	1016.6	1285.1	1383.8	1755.5	2010.4	2094.6
Hybrid	$f_{1,1}$	$f_{1,2}$	$f_{2,1}$	$f_{1,3}$	$f_{2,2}$	$f_{2,3}$	$f_{1,4}$	$f_{2,4}$	$f_{3,1}$	$f_{3,2}$
	284.8	541.1	985.4	1052.4	1139.2	1518.1	1794.0	2164.4	2173.6	2289.9

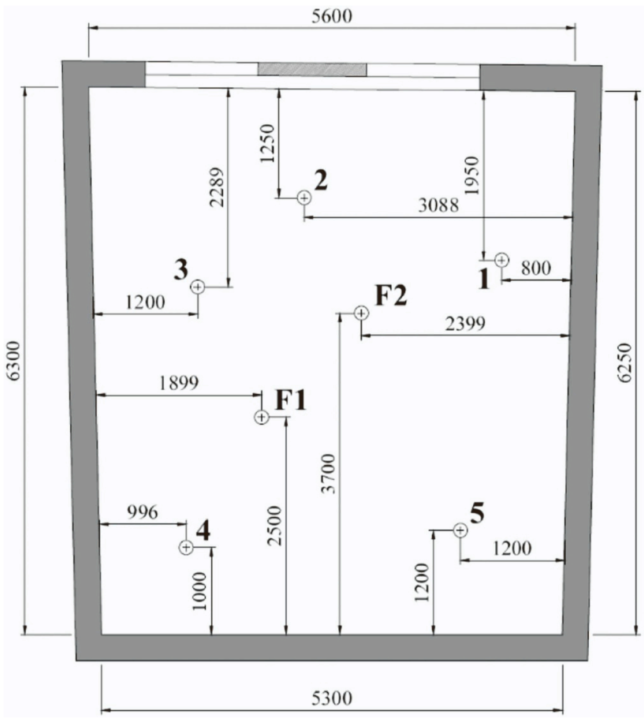

Fig. 7. Position of the microphones (1–5) and sound sources (F1 and F2) in the source chamber (average height of 3350 mm) (dimensions in mm).

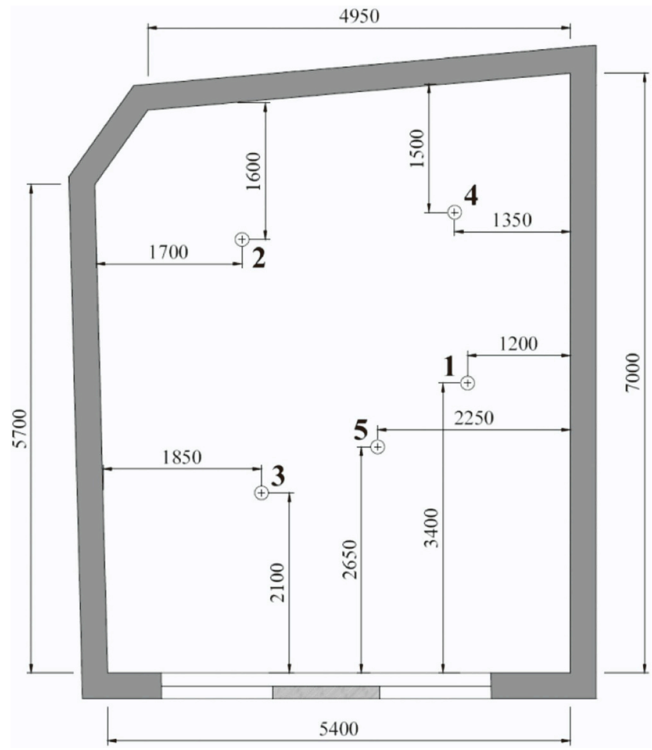

Fig. 8. Position of the microphones (1–5) in the receiving chamber (average height of 3150 mm) (dimensions in mm).

mineral wool with silicone seal around the panels.

According to ISO 10140–2 [26], the sound reduction indices in 1/3 octave bands (R) are calculated according to Eq. (2),

$$R = L_1 - L_2 + 10\bullet\log_{10}\frac{S}{A} \tag{2}$$

where L_1 is the energy average sound pressure level in the source room, in dB; L_2 is the energy average sound pressure level in the receiving chamber, in dB; S is the area of the test specimen, in m^2; and A is the equivalent sound absorption area in the receiving chamber, in m^2. The energy average sound pressure levels were calculated considering Eq. (3), as prescribed by ISO 140–4 [31],

$$L = 10\bullet\log_{10}\left(\frac{p_1^2 + p_2^2\ldots + p_n^2}{n\bullet p_0^2}\right) \tag{3}$$

where p_1, p_2, …, p_n are the root-mean-square pressures at n different microphone positions in the room and p_0 is the reference air pressure, equal to 2×10^{-5} Pa.

According to EN 12354–1 [32], the standardized level difference (D_{nT}) and the normalized level difference (D_n) can be calculated according to Eqs. (4) and (5), respectively,

$$D_{nT} = L_1 - L_2 + 10\bullet\log_{10}\frac{T}{T_0} \tag{4}$$

$$D_n = L_1 - L_2 + 10\bullet\log_{10}\frac{A}{A_0} \tag{5}$$

where T_0 is the reference reverberation time for dwellings of 0.5 s), and A_0 is the reference absorption area, taken as 10 m^2.

The determination of the reverberation time was performed according to ISO 354 [33] by placing the sound source in the receiving chamber in two different positions and considering five microphone positions in the receiving chamber (those depicted in Fig. 8). For each combination of sound source and microphone positions, two repetitions were considered. The reverberation times were calculated based on the average of all these measurements for each 1/3 octave frequency band ranging from 50 to 5000 Hz – the results obtained are presented in Table 2.

According to ISO 10140–5 [34], the reverberation time (T_r) of the chamber should be higher than 1 s and lower than $2\bullet(V/50)^{2/3} = 3.62$ s (V is the volume of the chamber, 122 m^3). Only for the 50 Hz and 63 Hz frequency band the reverberation time exceeds the normative limit. However, these frequency bands (plus the 80 Hz band) were not included in the airborne analysis of sound reduction indices. According to Sabine's equation, Eq. (6), the reverberation times can be related with the equivalent absorption area of the chamber as long as the sound absorption coefficient (α) is lower than 0.1:

$$T_r = \frac{0.161\bullet V}{A} \tag{6}$$

The equivalent absorption areas for each 1/3 octave frequency band are presented in Table 3.

The background noise was also registered in both chambers, but no correction to the results was needed, as the difference between the background noise pressure level and the pressure level at each chamber was far greater than 15 dB (maximum difference value for which ISO 10140–4 [30] requires a background noise correction).

3.3. Impact sound insulation tests

The impact sound pressure level tests performed according to ISO 10140–5 [34] require large acoustic chambers with standardized dimensions. Despite that, similar tests have been performed on a reduced test chamber (with an internal volume of 2.73 m^3) and results obtained from both standardized tests and *in-situ* measurements (two contiguous rooms of consecutive levels) for other types of specimens were very similar [25],[35]; thus giving confidence on the reliability of such test setup, whose details can be found in the referred works.

In the tests, the specimens were placed on top of the small-size test chamber, and were supported along the 10 cm thick chamber walls. A

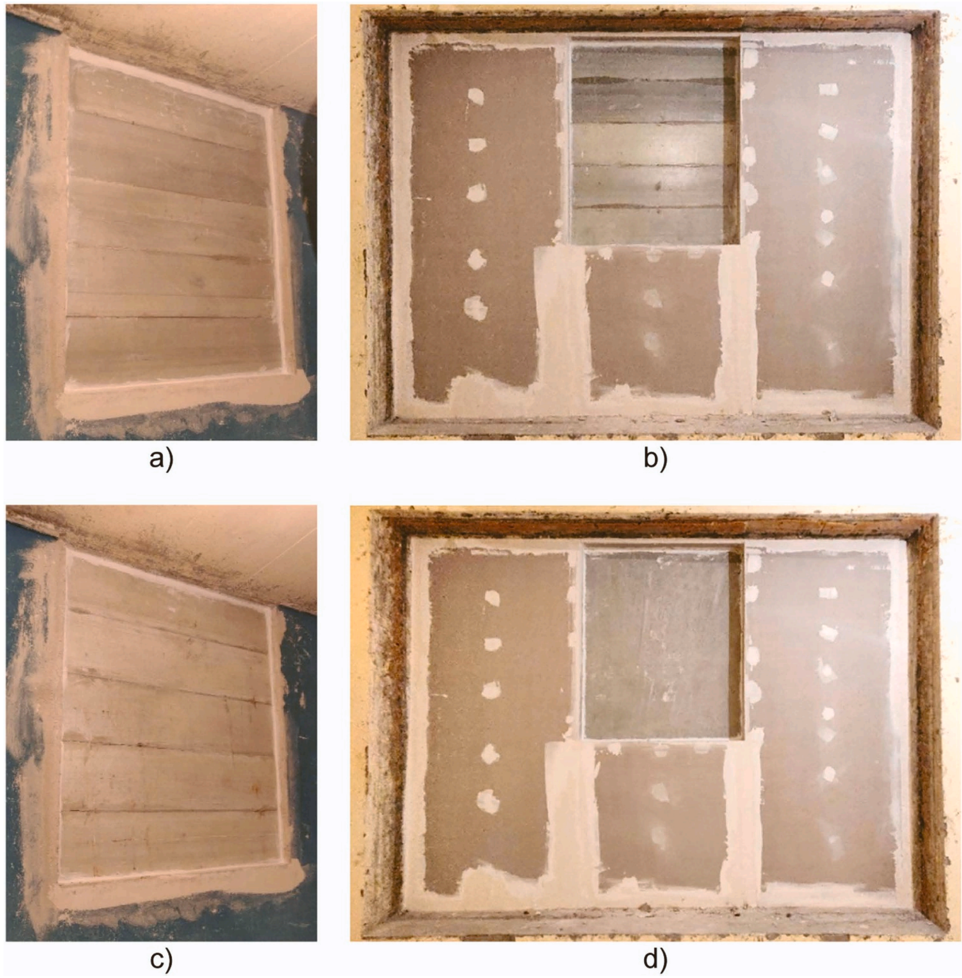

Fig. 9. Airborne sound transmission tests of the *EasyFloor* panels: a) receiving room view with the all-GFRP panel; b) source room view with the all-GFRP panel; c) receiving room view with the hybrid panel; d) source room view with the hybrid panel.

Table 2
Reverberation times of the receiving chamber per 1/3 octave frequency band.

f [Hz]	50	63	80	100	125	160	200	250	315	400	500
T [s]	4.65	4.04	3.31	3.26	2.63	2.81	2.64	2.54	2.54	2.53	2.41
f [Hz]	630	800	1000	1250	1600	2000	2500	3150	4000	5000	
T [s]	2.44	2.49	2.51	2.61	2.62	2.55	2.36	2.19	1.91	1.67	

Table 3
Equivalent absorption area of the receiving chamber per 1/3 octave frequency band.

f [Hz]	50	63	80	100	125	160	200	250	315	400	500
A [m^2]	4.20	4.84	5.89	5.99	7.41	6.95	7.41	7.68	7.69	7.72	8.09
f [Hz]	630	800	1000	1250	1600	2000	2500	3150	4000	5000	
A [m^2]	8.01	7.85	7.76	7.49	7.46	7.65	8.28	8.93	10.24	11.72	

resilient cork layer was placed between the panel and the chamber walls to reduce flanking transmissions. After placing the panel on top of the chamber, a thin silicone line was applied to the chamber-panel interface in order to guarantee the sealing between the two elements, thus further reducing flanking transmissions. The silicone was left to cure for a period of 24 hours.

The following equipment was used for the impact sound pressure level tests (Fig. 10): (i) a 4-channel data acquisition device, from *National Instruments*, model *NI USB 4431*; (ii) three ½'' microphones, from *GRAS* model *46 A*; and (iii) a *Brüel & Kjær* type *3207* tapping machine. The acquisition and processing of the signals during each test was performed using MATLAB software [36].

Inside the chamber, and following the provisions of ISO 10140–4 [30], the number of microphone positions was equal to the number of tapping machine positions. Five positions, labelled from A to E, are presented in Fig. 11 and were chosen with different distances to each orthogonal face of the chamber to minimize close-to-wall effects. However, the minimum distance of 0.7 m to any of the chamber boundary elements (defined in the standard) was not fulfilled, as the chamber dimensions were too small. Also, three different orientations of the tapping machine were considered for each position: (i) 0° (aligned with the webs of the panels); (ii) 45° (forming a 45° angle with the webs

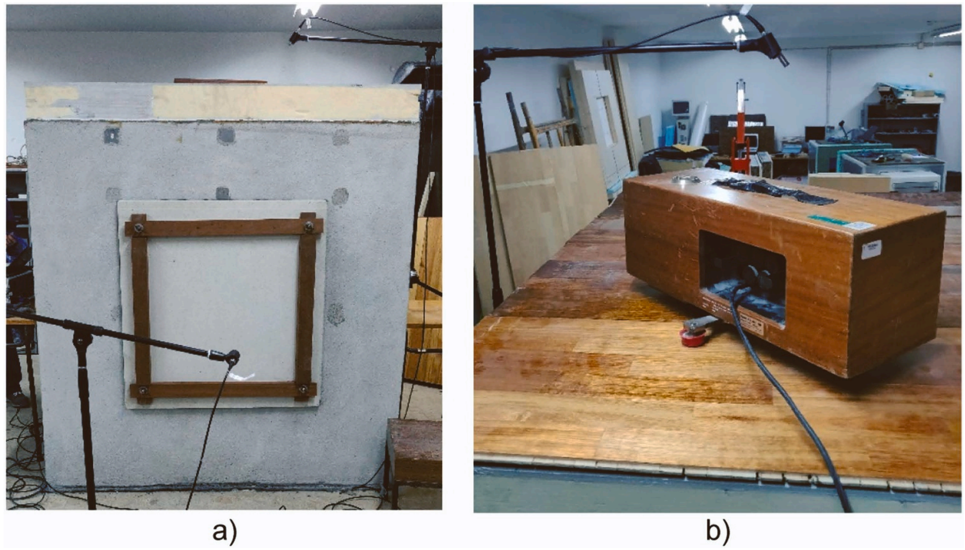

Fig. 10. Impact sound pressure level test setup: a) microphones outside the acoustic chamber; b) tapping machine.

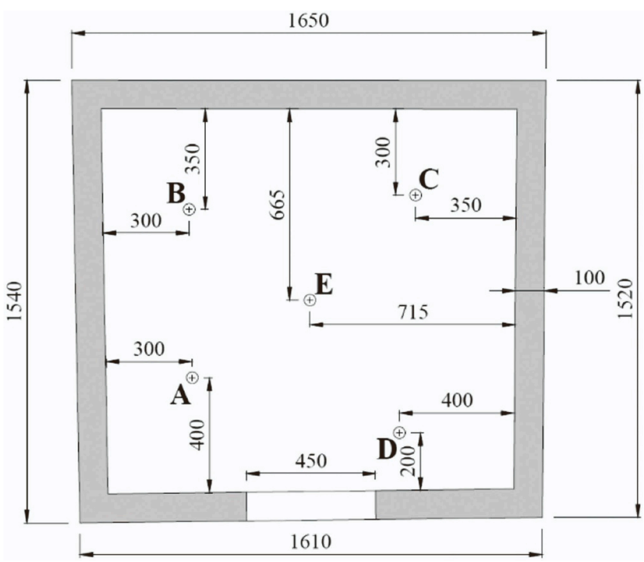

Fig. 11. Position of the microphones (A to E) inside the acoustic chamber (height = 1500 mm) (dimensions in mm).

of the panels), and (iii) 90° (perpendicular to the webs of the panels). For each tapping machine position, measurements were performed for the five different microphone positions. In total, 75 measurements were performed for each test (3 tapping machine orientations times 5 tapping machine positions times 5 microphone positions). Each measurement was taken for a period of 10 s, longer than the minimum of 6 s stated in ISO 10140–4 [30].

The pressure (p) was used to calculate the impact sound pressure level (L_i) using Eq. (7):

$$L_i = 20 \bullet \log_{10}\left(\left|\frac{p}{p_0}\right|\right) \tag{7}$$

After determining the energy average sound pressure level (L), according to Eq. (3), the normalized impact sound pressure level was then calculated using Eq. (8),

$$L_n = L_i + \log_{10}\frac{A}{A_0} \tag{8}$$

where L_i is the impact sound pressure level in dB and A_0 is the reference equivalent absorption area in m^2.

Corrections were introduced to reduce the contamination of the measured sound pressure level inside the chamber by airborne transmission following the procedure described in [25]. Indeed, it is known that in impact tests airborne transmission through weak elements of the test chamber may influence the final results; in the present case, these elements include the lateral door and also the tested floor specimen. For such correction, two microphones were placed outside the chamber to measure the outside pressure level: (i) one in front of the chamber door, at about 1 m of distance and aligned with the center of the door, and (ii) another one between the top of the slab and the ceiling (about 0.5 m from the top of the slab). The microphones that were placed outside the chamber and the tapping machine are presented in Fig. 10a and Fig. 10b, respectively. The sound pressure level due to the airborne sound generated by the impact source that crosses the floor and door elements ($L_{i\_airborne}$) was calculated from the energy average sound pressure level measured in front of the door (L_{out_door}) and the floor (L_{out_floor}), according to Eq. (9),

$$L_{i\_airborne} = 10 \bullet \log_{10}\left(\frac{1}{2}\left(10^{\frac{L_{out\_door} - D_{door}}{10}} + 10^{\frac{L_{out\_floor} - D_{floor}}{10}}\right)\right) \tag{9}$$

where D_{door} and D_{floor} are the uncorrected airborne sound insulation of the door and floor, respectively.

If $L_i - L_{i_{airborne}} < 10$ dB, then L_i is replaced by L_{i_impact} that corresponds to the sound pressure level due to impact sound, calculated according to Eq. (10).

$$L_{i\_impact} = 10 \bullet \log_{10}\left(10^{\frac{L_i}{10}} - 10^{\frac{L_{i\_airborne}}{10}}\right) \tag{10}$$

The correction due to background noise is performed in the same way as described for the airborne sound tests.

The effects of a typical floor covering on the impact sound pressure level were also analysed for both types of sandwich panels – all-GFRP and hybrid. For this analysis, a wooden floor covering composed of wood planks with thickness of 15 mm and mass of 10.5 kg/m^2, supported on a resilient cork layer, was applied to the top face of the specimens. The resilient cork layer had thickness of 5 mm, mass of 172 kg/m^3 and dynamic stiffness of 190 MN/m^3 [35]. Then, the impact sound pressure level test procedures were repeated for the specimen configuration with resilient floor covering. These tests allowed to calculate the reduction of impact sound pressure level (ΔL) according to EN ISO 12354–2 [37], as per Eq. (11),

$$\Delta L = L_{n0} - L_n \quad (11)$$

where L_{n0} and L_n are the normalized impact sound pressure level (in dB) in the absence and presence of floor covering, respectively.

Firstly, the all-GFRP sandwich panel was submitted to an impact sound pressure test without any floor covering (Fig. 12a). Then, the resilient floor covering was applied to the top face of the panel (Fig. 12b) and the test was repeated.

4. Results and discussion

4.1. Airborne sound reduction

Fig. 13 presents the one-third octave frequency spectrum of the experimentally determined airborne sound reduction of both types of *EasyFloor* web-core sandwich panels. Also, the results of a similar type of composite sandwich panel, but with homogeneous core *(RehabGFRP)*, are presented for comparative purposes. The *RehabGFRP* panel had an overall thickness of 134 mm, comprising two identical GFRP face sheets with 7 mm of thickness, and a rigid PUR foam core with thickness of 120 mm and density of $\rho_c = 87$ kg/m^3, presenting a weight of 37.2 kg/m^2. It is worth referring that this latter panel was tested in a normalized full-scale chamber, with 10 m^2 of plan area, and therefore experimental results are less affected by the floor modal behaviour than those obtained for the *EasyFloor*. Further details about the characterization of the acoustic behaviour of the *RehabGFRP* panel can be found in [38].

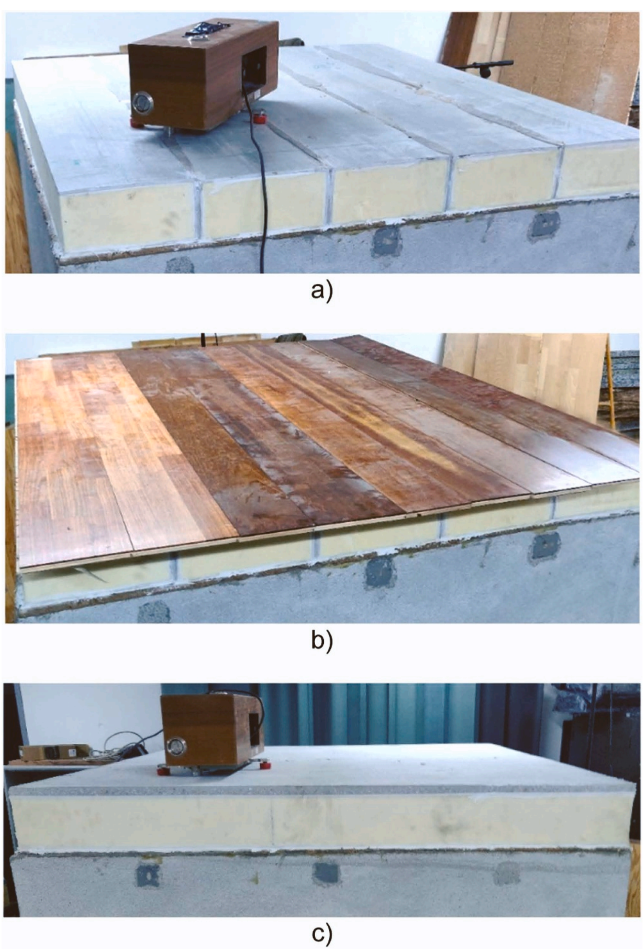

Fig. 12. Impact sound pressure test: a) all-GFRP sandwich panel (no covering) with tapping machine; b) all-GFRP sandwich panel with resilient floor covering; c) hybrid sandwich bare panel.

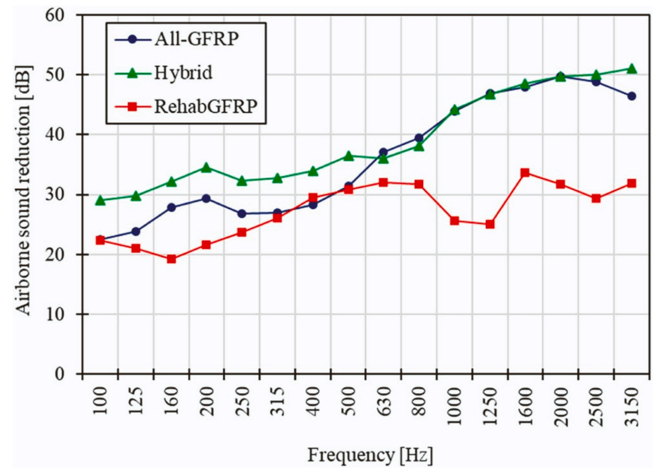

Fig. 13. Airborne sound reduction of the *EasyFloor* sandwich panels and the *RehabGFRP* panel.

The overall shape of the airborne sound reduction curves of the *EasyFloor* panels are quite similar, only showing differences for frequencies lower than 630 Hz. For the lowest frequency bands, the hybrid panel presents higher airborne sound reductions of about 5–6 dB when compared to the all-GFRP panel. It can be assumed that the composite sandwich panel controls the shape of the sound reduction curve, with the concrete top layer only increasing the noise reduction for frequency bands up to 630 Hz. It is also relevant to analyse the dips in the sound reduction curves, as they are usually related with resonant behaviour phenomena. The all-GFRP panel shows a first dip from 250 to 500 Hz, while the hybrid panel seems to present a double dip along a wider frequency range, from 250 to 800 Hz. Data given in Table 1 shows that the lowest values of modal density are obtained for the one-third octave frequency bands of 250 and 400 Hz for the all-GFRP panel, whereas for the hybrid panel the lowest values occur at 315, 500 and 1000 Hz, which explains the observed experimental behaviour. The all-GFRP panel also presents the initiation of a dip in the 3150 Hz frequency band. Regarding the *RehabGFRP* panel, a first dip occurs at the 160 Hz frequency band, with a second and third dips occurring at 1000–1250 and 2500 Hz, respectively. The differences on the overall shape of the airborne sound reduction spectra of the *EasyFloor* and *RehabGFRP* panels might be related with the test methods and size of the samples, together with the presence of GFRP webs on the *EasyFloor* panels, as these vertical (shear) strengthening elements of the core entail a significantly diverse structural system, which responds differently to acoustic waves.

The application of the rating method described in EN 717–1 [39] yielded a weighted sound reduction index R_w (C, C_{tr},$C_{100\text{–}5000}$, $C_{\text{tr}100\text{–}5000}$) = 38 (-1, −5, −1, −5) dB for the all-GFRP sandwich panel. For the hybrid sandwich panel, the same rating method yielded a R_w (C, C_{tr},$C_{100\text{–}5000}$, $C_{\text{tr}100\text{–}5000}$) = 41 (-1, −3, 0, −3) dB, which is in agreement with the expected improvement after doubling the floor mass. The *EasyFloor* panel's weighted sound reduction indexes compare to a much lower value of the *RehabGFRP* of R_w = 32 dB, which has a slightly lower mass per unit area than the all-GFRP *EasyFloor* panel.

4.2. Impact sound insulation tests

Fig. 14 presents the experimentally measured one-third octave spectrum of the impact sound pressure level for the all-GFRP sandwich panel with and without a resilient floor covering. Both specimens present a similar trend throughout the frequency spectrum, which shows how the panel governs the noise transmission from the tapping machine to the interior of the chamber, as expected. The addition of the resilient

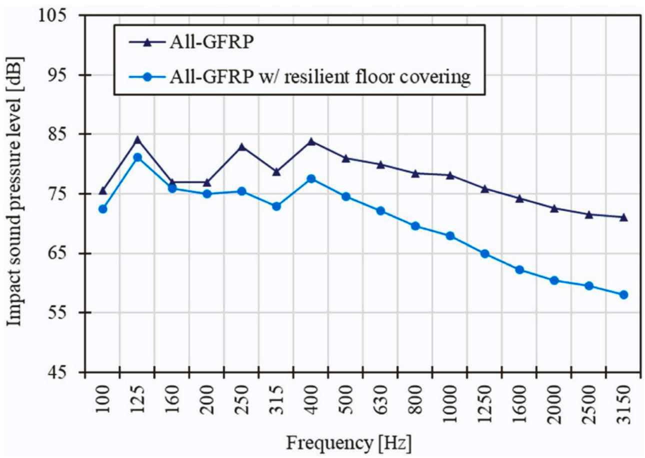

Fig. 14. Comparison of the impact sound pressure level of the all-GFRP sandwich panel with and without a resilient floor covering.

floor covering provided gains in terms of insulation of the impact noise generated by the tapping machine, also as expected. The specimen without floor covering presented the maximum impact sound pressure level at frequencies of 125, 250 and 400 Hz, thus confirming the occurrence of a resonant behaviour in the enclosure at 125 Hz (the first acoustic normal modes in each direction occur at frequencies in the range 105–114 Hz) and of a resonant behaviour in the plate at 250 and 400 Hz, combined with a plate-room coupling effect [40], which is more significant at the 250 Hz ($f_{1,1}$ = 254.1 Hz and $f_{0,0,(2)}$ = 228.1 Hz) than at the 400 Hz one-third octave frequency band ($f_{1,2}$ = 438.9 Hz and $f_{0,1,(4)}$ = 468.1 Hz). After the 400 Hz one-third octave frequency band, the impact sound pressure level decreased at rates of about 4 dB/octave and 7 dB/octave for the specimens without and with floor covering, respectively. The application of the rating method described in EN 717–2 [41] yielded a weighted normalized impact sound pressure level of $L_{n,w}$ = 81 dB for the all-GFRP sandwich panel without floor covering. The addition of a resilient floor covering reduced the overall impact sound generated by the tapping machine and yielded a $L_{n,w}$ = 72 dB, which reflects an improvement of 9 dB in the normalized single value ($L_{n,w}$).

The experimentally measured one-third octave spectra of the impact sound pressure level for the hybrid sandwich panel with and without a resilient floor covering are presented in Fig. 15. The specimen without floor covering presented the maximum impact sound pressure level at frequencies of 125, 250 and 630 Hz. This confirms, again, the occurrence of a resonant behaviour in the enclosure at 125 Hz, and of a resonant behaviour in the plate at 250 and 630 Hz, combined with a plate-room coupling effect; this effect is, once more, stronger at the 250 Hz ($f_{1,1}$ = 284.8 Hz and $f_{0,0,(2)}$ = 228.1 Hz) than at the 630 Hz one-third octave frequency band ($f_{1,2}$ = 541.1 Hz and $f_{0,1,(5)}$ = 579.8 Hz).

The results of the two specimens are almost similar up to the 315 Hz frequency band, thus confirming the predominance of the room behaviour over that of the plate mainly below 250 Hz; for higher frequencies, the specimen with a floor covering presented increasingly lower impact sound pressure levels. From that frequency band on, the impact sound pressure level continuously decreased. The application of the rating method described in EN 717–2 [41] yielded a weighted normalized impact sound pressure level of $L_{n,w}$ = 85 dB for the hybrid sandwich panel, which is slightly worse than that of the all-GFRP sandwich panel, mainly due to a significant modal behaviour up to 2000 Hz with resonances leading to higher sound pressure levels above 500 Hz. This discrepancy is related to the fact that in the all-GFRP panel the top face sheet is less stiff than in the hybrid panel, increasing the panel eigenfrequencies, and possibly because the tapping machine generate impacts mainly located in more damped areas (*i.e.*, above the PUR foam and not above the GFRP webs). Furthermore, in the hybrid panel, the concrete layer allows for a more efficient distribution of energy to the ribs, due to the increased stiffness of the top (hybrid) layer. However, the addition of a resilient floor cover to the hybrid panel yielded a $L_{n,w}$ = 69 dB, which is lower than the corresponding value for the all-GFRP panel; these results are in agreement with the predictions obtained from the mass law together with the reciprocity principle [42]. In this case, the resilient floor cover promoted a ΔL_w of 16 dB, which is almost twice the value of the effect on the all-GFRP panel. To better depict the effects of the resilient floor covering on the two types of *EasyFloor* panels tested, Fig. 16 presents a comparison of the reduction of impact sound pressure level. As stated, the floor covering had a higher effect on the hybrid panel, which is illustrated by the higher overall slope of the impact sound pressure level reduction in the hybrid panel for frequency bands higher than 500 Hz compared to the all-GFRP panel; for this range, the floor covering driving-point impedance is likely to be lower due to a higher coupling with the sandwich panel than that occurring in the hybrid panel, thus yielding impedance values lower than those of the impact source at higher frequencies.

Fig. 17 presents a comparison of the one-third octave spectrum of the impact sound pressure level of the *EasyFloor* web-core sandwich panels – all-GFRP (41.7 kg/m^2) and hybrid (89.7 kg/m^2) – with the *RehabGFRP* homogenous-core composite sandwich panel (37.2 kg/m^2), which was tested in a normalized full-scale chamber, with 10 m^2 of plan area.

The *RehabGFRP* panel (homogeneous-core, no GFRP webs) presents the worst overall performance, whereas the hybrid sandwich panel

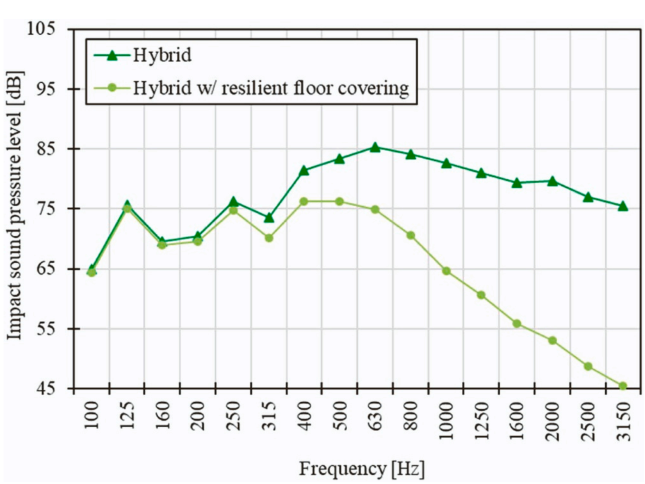

Fig. 15. Comparison of the impact sound pressure level of the hybrid sandwich panel with and without a resilient floor cover.

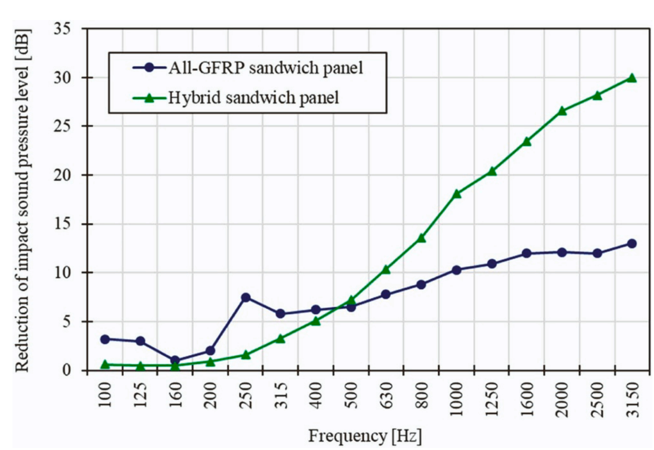

Fig. 16. Reduction of impact sound pressure level provided by the resilient floor cover.

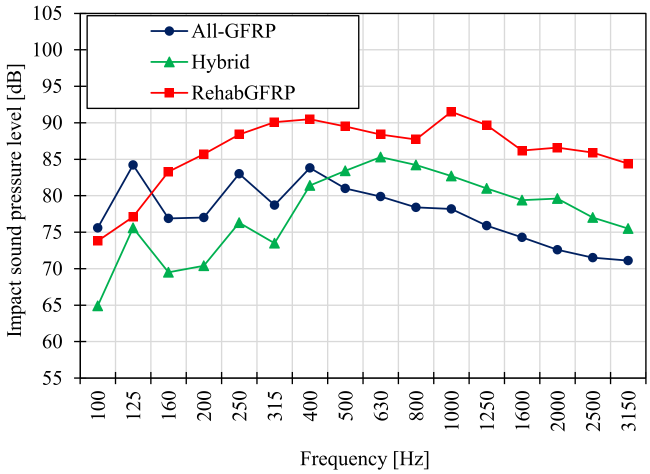

Fig. 17. Comparison of impact sound pressure level of various solutions.

exhibits the best performance up to the 1000 Hz frequency band and the all-GFRP panel presents the best performance from that frequency band onwards. Again, the differences on the overall shape of the impact sound pressure level spectra of the *EasyFloor* and *RehabGFRP* panels might be related with the test methods and size of the samples, together with the presence of GFRP webs on the *EasyFloor* panels.

5. Analytical study

5.1. Models

Several simplified analytical models have been proposed in order to predict the sound reduction characteristics of sandwich panels in an expedite manner. All these models include some combination of the mass law and the effect of different resonant frequencies that might occur in typical sandwich panels. Three different resonant frequencies are usually stated: a) natural frequencies (f_n), which depend on the bending stiffness, the mass and the dimensions of the panel; b) critical frequency (f_c), that is related solely to the mass and the bending stiffness; and c) dilatation frequency (f_{dil}) or mass-spring-mass resonance frequency, which is typically related to the mass of the face sheets and the stiffness of the core.

In this study, the following analytical models were assessed: (i) Sharp's model [28]; (ii) Krakers' model [19]; and (iii) Ballagh's model [20]. Table 4 highlights the application range of the analytical models assessed herein, namely the panel type, the type of materials and the panel properties considered as input.

Given the unavailability of an experimentally determined value, a value of 0.15 was considered for the loss factor of the rigid PUR foam based on [24]. The PUR loss factor has been reported to vary between 0.05 and 0.15 [43] and higher values have also been used in previous studies. After comparison of the results obtained for a loss factor variation between these limits of 0.05 and 0.15, it was concluded that the best fitting to the data in this work would result from a loss factor of 0.15. Table 5 presents a summary of the dilatation frequencies of the *EasyFloor* panels calculated with different methods, which led to substantial differences in the value of f_{dil}. Based on data from the literature [44,45], the elasticity modulus and Poisson ratio of the PUR foam core were considered to be 25 MPa and 0.3, respectively. In the case of the hybrid sandwich panels, f_{dil} was adapted in order to consider the difference between the upper and lower face sheets.

As the critical frequency varies with the wave direction, due to orthotropy, the minimum value was considered in calculations, *i.e.*, that for the transverse direction.

Table 4
Analytical models application range.

Analytical model	Sharp [28]	Krakers [19]	Ballagh [20]
Panel type	Infinite single panels and laminated panels	Finite sandwich panels	Sandwich panels
Type of materials	Homogeneous isotropic materials	Homogeneous isotropic materials	Homogeneous isotropic materials
Panel properties considered as input	Mass, loss factor and critical frequency	Mass, radiation coefficient, loss factor, f_n, f_c and f_{dil}	Mass, fraction of critical damping and f_{dil}

Table 5
Comparison of the dilatation frequencies (f_{dil}) according to the different models.

Type of *EasyFloor Panel*	f_{dil} [Hz]		
	Krakers [19]	Wawrzynowicz [24]	Ballagh [20]
All-GFRP	536.6	1071.8	994.7
Hybrid	303.4	469.8	759.1

5.2. Comparison with experiments

Fig. 18 compares the analytical predictions obtained from Sharp's model with the experimental results for the all-GFRP and hybrid sandwich panels. Based on the conclusions of Santos *et al.* [25], two variations of the original Sharp's model were considered, replacing the critical frequency (f_c) by the first natural frequency ($f_{1,1}$) or the dilatation frequency (f_{dil}), due to the poor accuracy of the results obtained with the original model, which considers f_c as the resonant frequency. The dilatation frequency was calculated according to Krakers [19] formulation.

As previously stated, the consideration of the critical frequency as the main resonant frequency, according to Sharp's model, leads to an overall shape of the noise reduction curve that differs significantly from the results obtained experimentally; this shows that for low critical frequencies (84.8–157.0 Hz in the all-GFRP panel and 78.6–119.8 Hz in the hybrid panel), mass law deviations are controlled by natural frequencies corresponding to bending vibration modes and dilatational resonances. Regarding the all-GFRP panel, considering the natural frequency or the dilatation frequency leads to analytical predictions that are close to the experimental results, with the consideration of the natural frequency as the main resonant frequency capturing very well the first dip in the noise reduction curve. Similar conclusions can be drawn for the hybrid panel; for this panel, Sharp's model considering either the first natural frequency or the dilatation frequency reproduces very accurately the first dip in the airborne sound reduction curve, but it does not capture the second one.

Fig. 19 compares the experimental results with the estimated values obtained from the Krakers analytical model considering the dilatation frequency predicted according to Krakers, Ballagh and Wawrzynowicz. The estimates provided by these analytical methods include pronounced noise reduction dips, which correspond, from low to high frequencies, to the critical frequency, the first bending resonance and the dilational resonance. Both the critical frequency and the natural frequency corresponding to the first bending vibration mode seem to be correctly estimated, mainly for the all-GFRP panel, although the magnitude of the analytical dips is much higher than that obtained experimentally for both types of panels, which might indicate that the considered loss factor is low (Fig. 20 shows the sound reduction spectra obtained for a core loss factor of 0.15). The estimated dilatational frequencies (Table 5), however, not only differ significantly from model to model but also differ from measurements; in fact, Ballagh's and Wawrzynowicz's models seem to overestimate the dilatation frequency, whereas Krakers' model seems to underestimate this value. Furthermore, the model clearly

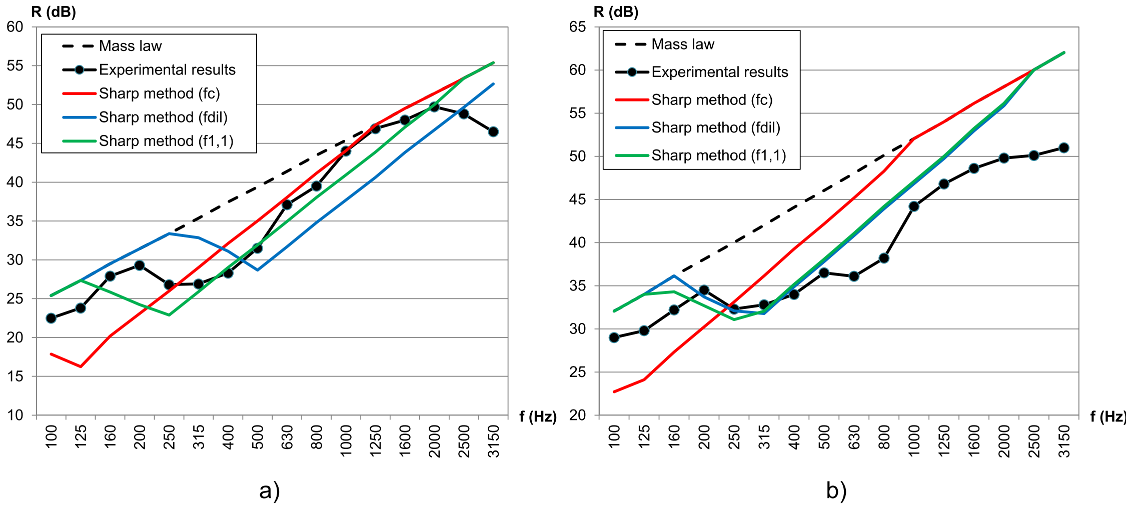

Fig. 18. Comparison of Sharp's analytical model with experimental results: a) all-GFRP panel; b) hybrid sandwich panel.

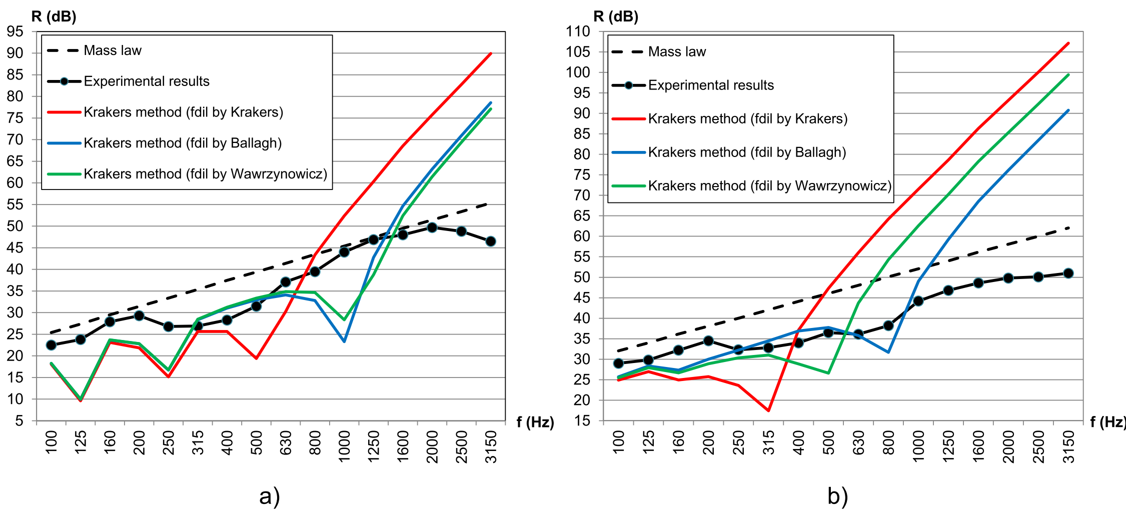

Fig. 19. Comparison of Krakers' analytical model (considering a core loss factor of 0.05) with experimental results: a) all-GFRP panel; b) hybrid sandwich panel.

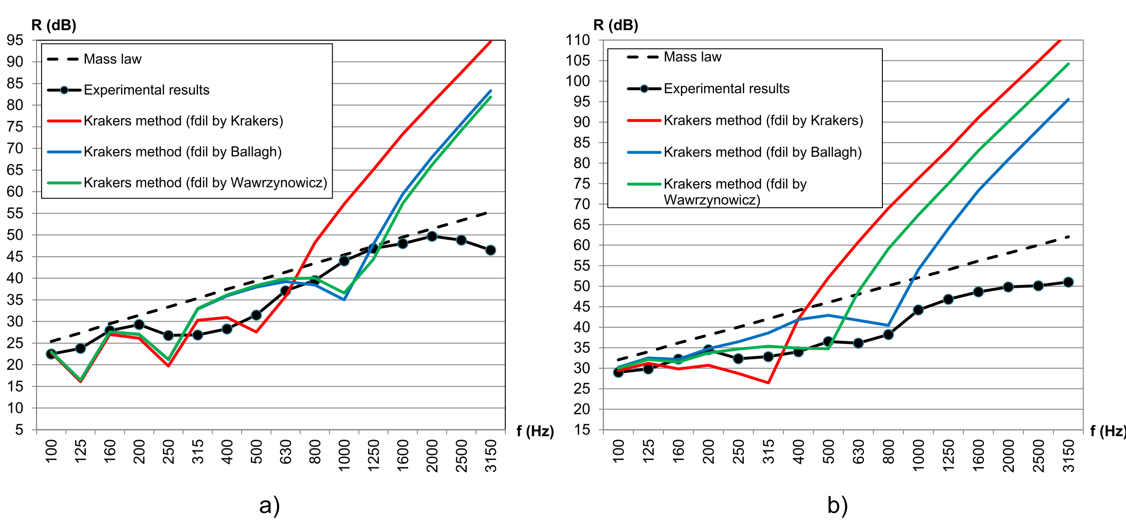

Fig. 20. Comparison of Krakers' analytical model (considering a core loss factor of 0.15) with experimental results: a) all-GFRP panel; b) hybrid sandwich panel.

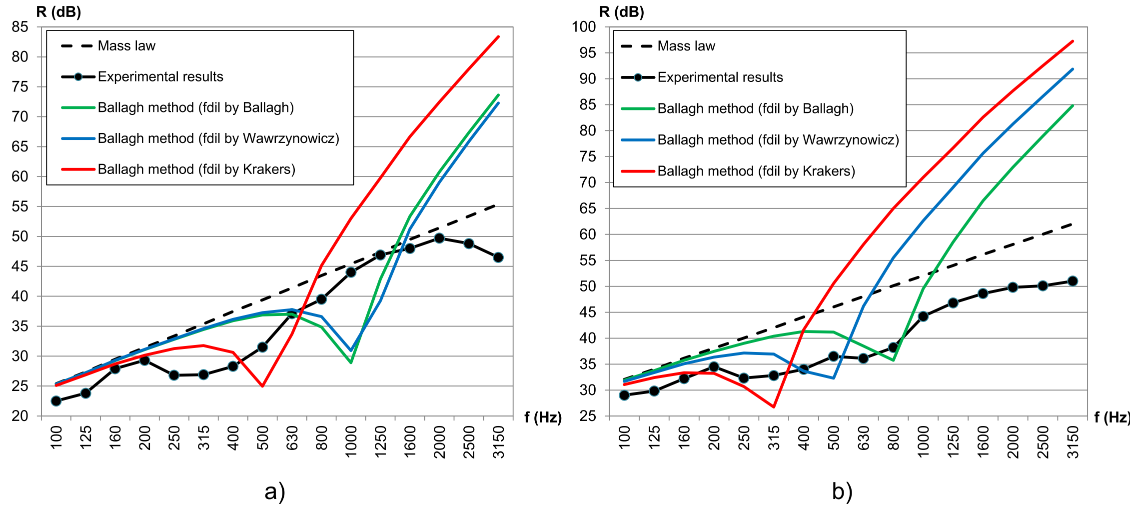

Fig. 21. Comparison of Ballagh's analytical model with experimental results: a) all-GFRP panel; b) hybrid sandwich panel.

overestimates the sound reduction of both panels at higher frequencies (above 800 Hz) for all the considered dilatation frequencies, which is due to the fact that the dilatation term of the model assumes very high values for this frequency bands region, leading to sound reduction values above those provided by mass law.

Fig. 21 presents a comparison of the predictions obtained with Ballagh's analytical model with the experimental results of the *EasyFloor* composite sandwich panels. A value of 0.075 was considered for the critical damping coefficient ($\xi=\eta/2=0.15/2$) according to the author's recommendations [20]. Similarly to the results of Krakers' model, and because this model is based on the transmissibility of a damped mass-spring-mass system, it largely overestimates sound reduction at the higher 1/3 octave frequency bands. Again, with a core loss factor of 0.15, the dip in the estimated sound reduction index is significantly closer to the experimental results, yet missing the dips corresponding to both the critical frequency and the natural frequencies associated to the first bending vibration modes.

To sum up, Sharp's model seems to present the most adequate predictions when considering the natural and dilatation frequencies as the critical frequency, while the original model retrieves a sound reduction spectrum that largely differs from the experimental results. Krakers' and Ballagh's analytical models both fail to retrieve accurate predicitons of the noise reduction at the higher frequency bands. These models assume that the ressonant behaviour at the dilatation frequency is responsible for damping phenomena at frequencies much higher than f_{dil}, which does not seem to be correct, based on the experimental results. These findings highlight the complexity of this type of structural floor systems (web-core sandwich panels combining GFRP webs and PUR foam core) regarding the prediction of their acoustic response using simple and expeditious analytical formulations.

From the presented results, a possible alternative for the prediction of the airborne sound insulation of this type of system seems to be a hybrid model, which follows Krakers' theoretical model at lower frequencies, up to the dilatational frequency, and then accounts for the higher frequencies using Sharp's approach. This, however, should be investigated in more detail in future studies.

6. Design and compliance with regulation

The main envisaged application of the developed sandwich panels is the rehabilitation of degraded wooden floors in old buildings. Therefore, one key aspect about the acoustic requirements considered in the development of such solution was to ensure a better acoustic insulation performance than that of the original light timber floors, comprised of joists and planks, which typically present poor acoustic performance, especially when compared with heavier and more recent building floor systems, such as reinforced concrete, steel-concrete composite and beam-and-block floor systems [46]. However, it is hard to quantify the acoustic properties of a typical light timber floor, as the structure, the materials and architecture can vary significantly from case to case. In this sense, the objectives of the *EasyFloor* project regarding the acoustic insulation properties of the developed sandwich panel floor systems were to meet, for all-GFRP and hybrid panels, the Portuguese acoustic legal requirements for rehabilitation of residential buildings, which are 3 dB lower than the requirements for new construction [47], reduced by 12 dB in the case of airborne sound and increased by 21 dB in the case of impact sound.

Building comfort requirements for housing and office buildings are strict and must be fulfilled in new construction, so mitigation measures may need to be adopted when composite sandwich panels are used in that scenario. In Portugal, such requirements are the Weighted Standardized Level Difference, $D_{nT,w} > 50$ dB, and the Weighted Normalized Impact Sound Pressure Level, $L'_{nT,w} \leq 60$ dB [48], for building floors. Legal requirements for airborne sound transmission can be defined by different indicators across the world (R_w, $D_{n,w}$, $D_{nT,w}$, or *FSTC*), which normally are in the range of 45–55 dB in most countries [30]. Impact sound transmission is also described by different indicators ($L'_{n,w}$, $L'_{nT,w}$), which can vary significantly (range of 43–68 dB), although most countries consider limits below 60 dB [49,50]. As the different insulation descriptors used assume roughly the same value in laboratory, they can be used for comparison with R_w and $L_{n,w}$ estimates with no need for further conversion. Table 6 presents a compilation of the acoustic insulation requirements considered in the development and analysis of the *EasyFloor* sandwich panel floor systems.

Table 6
Acoustic insulation requirements.

Sound transmission	Design objectives		Legal requirements (new construction)	
	All-GFRP	Hybrid	Portugal	Other countries
Airborne sound reduction	$R_w > 38$ dB	$R_w > 38$ dB	$D_{nT,w} > 50$ dB	R_w, $D_{n,w}$, $D_{nT,w}$, *FSTC* > 45–55 dB
Impact sound pressure level	$L_{n,w} < 81$ dB	$L_{n,w} < 81$ dB	$L'_{nT,w} < 60$ dB	$L'_{n,w}$, $L'_{nT,w} < 43$–68 dB

Table 7
Experimentally determined sound insulation indices of the *EasyFloor* panels.

Noise index	*EasyFloor Panels*		Design objectives
	All-GFRP	Hybrid	All-GFRP and hybrid
R_w (dB)	38	41	38
$L_{n,w}$ (dB)	81[a] / 72[b]	85[a] / 69[b]	81

[a] specimen without resilient floor covering.
[b] specimen with resilient floor covering.

Table 7 compares the design goals and the values obtained experimentally. The all-GFRP *EasyFloor* panel meets the design requirements for the airborne sound reduction index and impact sound pressure level, while the hybrid panel only meets the latter with the addition of a resilient floor covering. These panels would also meet the Portuguese building comfort requirements for new construction with the consideration of typical additional constructive elements, which in this context can be considered as noise mitigation measures, such as false ceilings with one inner layer of mineral wool and a resilient floor covering (note that such a false ceiling would typically increase R_w by 10–15 dB and decrease $L_{n,w}$ by 5 dB). With such mitigation measures, it would be possible to achieve R_w and $L_{n,w}$ values of 53 dB and 67 dB, respectively, for the all-GFRP panel. For the hybrid panel, the expected improved R_w and $L_{n,w}$ values would be 56 dB and 62 dB, respectively. In this case, both panels would possibly meet *in situ* sound insulation legal requirements for airborne and impact sound. However, these predictions need to be confirmed in future studies.

7. Conclusions

This paper described the results of full-scale standardized acoustic experiments performed on the web-core all-GFRP and GFRP-concrete hybrid *EasyFloor* sandwich panels. The tests were carried out in acoustic reverberation chambers in order to characterize their acoustic insulation properties to both airborne and impact sounds. The effect of a floor covering with a resilient layer on the impact sound pressure level of the tested specimens was also experimentally assessed.

One-third octave frequency band spectra of the impact sound pressure level and airborne sound reduction were determined for the panels. Weighted normalized impact sound pressure levels ($L_{n,w}$) of 72 dB and 81 dB were determined for the all-GFRP sandwich panel, with and without a resilient floor covering, respectively; while for the hybrid sandwich panel, those values were 69 dB and 85 dB. Weighted airborne sound reduction indices (R_w) of 38 dB and 41 dB were obtained for the all-GFRP and hybrid panels, respectively.

The experimentally determined airborne sound reduction spectra of the panels were compared with predictions obtained from three different analytical models typically applied to sandwich panels. Sharp's model provided the most accurate results when considering the natural and dilatation frequencies replacing the critical frequency to characterize deviations to mass law. The results obtained show that models developed for web-core composite sandwich panels fail to retrieve accurate predicitons of the sound reduction. Those models, namely Krakers' and Ballagh's, assume that the ressonant behaviour at the dilatation frequency is responsible for damping phenomena at frequencies much higher than f_{dil}, and the experimental results seem to suggest that this assumption is not correct for the type of panels studied herein.

The findings of this analytical and experimental study show how complex these web-core sandwich panel floor systems are in terms of predicting their acoustic response with simple and expeditious analytical formulations.

The final part of the paper presented an assessment about the compliance of the normalized airborne and impact sound indices determined experimentally with the design and regulatory requirements. This assessment showed that even without mitigation measures it should be possible to meet the objectives put forward in the design stage of the *EasyFloor* project. However, to apply the panels in new construction, where building comfort requirements are stricter, mitigation measures are needed to improve the sound insulation of these floor solutions. For example, adding false ceilings with one inner layer of mineral wool and applying a resilient floor covering could potentially allow meeting these regulatory requirements. In any case, further studies are required to experimentally confirm these predictions.

In the scope of the *EasyFloor* project, the performance of the proposed building floor system was assessed with respect to other aspects, namely structural behaviour, thermal performance and fire reaction and fire resistance behaviour [51,52]. It was shown that it is possible to fulfil building code requirements provided that appropriate passive fire protection systems are adopted, including insulation boards, either adherent to the bottom face sheet of the panels or forming an air cavity. As mentioned above, such fire protection solutions can also be used to improve the acoustic performance of the panels."

CRediT authorship contribution statement

Luis Godinho: Writing – review & editing, Resources, Investigation, Formal analysis. **Pedro Santos:** Writing – review & editing, Writing – original draft, Methodology, Investigation, Formal analysis. **Miguel Proença:** Writing – original draft, Visualization, Methodology, Investigation, Formal analysis, Data curation. **José Sena-Cruz:** Writing – review & editing, Project administration, Methodology, Conceptualization. **Mário Garrido:** Writing – review & editing, Supervision, Methodology, Investigation, Formal analysis, Conceptualization. **Joao R. Correia:** Writing – review & editing, Supervision, Resources, Project administration, Methodology, Investigation, Conceptualization. **Albano Neves e Sousa:** Writing – review & editing, Supervision, Methodology, Investigation, Formal analysis, Conceptualization.

Declaration of Competing Interest

The authors declare that they have no known competing financial interests or personal relationships that could have appeared to influence the work reported in this paper.

Data availability

Data will be made available on request.

Acknowledgements

This work was partly financed by FCT / MCTES through national funds (PIDDAC) through the R&D Unit Civil Engineering Research and Innovation for Sustainability (CERIS), reference UIDB/04625/2020 (doi.org/10.54499/UIDB/04625/2020), and under the R&D Unit Institute for Sustainability and Innovation in Structural Engineering (ISISE), under reference UIDB/04029/2020 (doi.org/10.54499/UIDB/04029/2020), and under the Associate Laboratory Advanced Production and Intelligent Systems ARISE under reference LA/P/0112/2020. This work is part of the research project "EasyFloor – Development of composite sandwich panels for rehabilitation of building floors", involving the company ALTO – Perfis Pultrudidos, Lda., CERIS/Instituto Superior Técnico and ISISE/University of Minho, supported by FEDER funds through the Operational Program for Operational Program for Competitiveness and Internationalization (POCI) and the Portuguese National Innovation Agency (ANI) – project no. 3480 (POCI-01–0247-FEDER-003480). The authors would like to acknowledge to company Tecnipor for the support provided, namely in providing and casting the concrete layer of the hybrid panels. The first author was supported by FCT through PhD scholarship SFRH/BD/145542/2019.

References

[1] J.M. Davies, Lightweight Sandwich Construction, Blackwell Science, Oxford, 2001.
[2] D. Zenkert, The Handbook of Sandwich Construction, Engineering Materials Advisory Services, EMAS, Worcestershire, 1997.
[3] V. Birman, G.A. Kardomateas, Review of current trends in research and applications of sandwich structures, Compos. B Eng. 142 (2018) 221–240.
[4] D.J.L. Kennedy, R.A. Dorton, S.D.B. Alexander, The sandwich plate system for bridge decks, Pittsburgh, : Proc. 2002 Int. Bridge Conf. (June 2002).
[5] R.B. Vincent, A. Ferro. A new orthotropic bridge deck: design, fabrication and construction of the Shenley Bridge incorporating an SPS orthotropic bridge deck, in: Proceedings of the 2004 Orthotropic Bridge Conference, August, 2004. Sacramento.
[6] D.K. Harris, T. Cousins, T.M. Murray, E.D. Sotelino, Field investigation of a sandwich plate system bridge deck, J. Perform. Constr. Facil. 22 (5) (2008) 305–315.
[7] Intelligent Engineering. The Grand Pier. Rehabilitation of the Weston Super Mare Pier (n.d.), November, 2009. UK, ⟨http://www.ie-sps.com/resources/IE-SPS-Project-Portfolio.pdf⟩. available online.
[8] Intelligent Engineering. Carnegie Hall South & North Tower. Renovation of a mezzanine Floor in Carnegie Hall South Tower and Floor Additions in the North Tower (n.d.), 2011. Manhattan, NY, USA, ⟨http://www.ie-sps.com/resources/IE-SPS-Project-Portfolio.pdf⟩. available online.
[9] S.T. Freitas, H. Kolstein, F. Bijlaard, Sandwich system for renovation of orthotropic steel bridge decks, J. Sandw. Struct. Mater. 13 (3) (2010) 279–301.
[10] J.R. Correia, M. Garrido, J.A. Gonilha, F.A. Branco, L.G. Reis, GFRP sandwich panels with PU foam and PP honeycomb cores for civil engineering structural applications: effects of introducing strengthening ribs, Int. J. Struct. Integr. 3 (2) (2012) 127–147.
[11] A. Fam, T. Sharaf, Analysis of large scale cladding sandwich panels composed of GFRP skins and ribs and polyurethane foam core, Thin-Walled Struct. 71 (2013) 91–101.
[12] T. Keller, C. Haas, T. Vallée, Structural concept, design and experimental verification of a GFRP sandwich roof structure, J. Compos. Constr. 14 (4) (2008) 454–468.
[13] M. Garrido, J.F.A. Madeira, M. Proença, J.R. Correia, Multi-objective optimization of pultruded composite sandwich panels for building floor rehabilitation, Constr. Build. Mater. 198 (2019) 465–478.
[14] M. Proença, A. Neves e Sousa, M. Garrido, J.R. Correia, Acoustic performance of composite sandwich panels for building floors: Experimental tests and numerical-analytical simulation, J. Build. Eng. 32 (2020) 101751.
[15] J. Nurzynski, L. Nowotny, Acoustic performance of floors made of composite panels, Materials *16* (2023) 2128.
[16] J.R. Correia, S. Cabral-Fonseca, F.A. Branco, J.G. Ferreira, M.I. Eusébio, M. P. Rodrigues, Durability of pultruded glass-fiber-reinforced polyester profiles for structural applications, Mech. Compos. Mater. 42 (4) (2006) 325–338.
[17] S. Cabral-Fonseca, J.R. Correia, M.P. Rodrigues, F.A. Branco, Artificial accelerated ageing of GFRP pultruded profiles made of polyester and vinylester resins: characterisation of physical–chemical and mechanical damage, Strain 48 (2) (2012) 162–173, 2012.
[18] V. D'Alessandro, G. Petrone, F. Franco, S. De Rosa, A review of the vibroacoustics of sandwich panels: models and experiments, J. Sandw. Struct. Mater. 15 (5) (2013) 541–582.
[19] L. Krakers. Parametric fuselage design - Integration of mechanics and acoustic & thermal insulation. PhD thesis in Aerospace Engineering. Delft University of Technology, Faculty of Aerospace Engineering, Netherlands, 2009.
[20] K. Ballagh, Adapting simple prediction methods to sound transmission of lightweight foam cored panels, Build. Acoust. 17 (4) (2010) 269–276.
[21] S. Patinha, F. Cunha, R. Fangueiro, S. Rana, F. Prego, Acoustical behavior of hybrid composite sandwich panels, Key Eng. Mater. 634 (2015) 455–464.
[22] R.M. Garay, N. Pino, G. acoustic behavior in three types of housing: brick social housing, structural insulated panel (SIP) emergency housing and mediagua emergency housing, Rev. De. la ConstruccióN. 18 (1) (2019) 96–110.
[23] G. Petrone, V. D'Alessandro, F. Franco, S. De Rosa, Numerical and experimental investigations on the acoustic power radiated by aluminium foam sandwich panels, Compos. Struct. 118 (2014) 170–177.
[24] A. Wawrzynowicz, M. Krzaczek, J. Tejchman, Experiments and FE analyses on airborne sound properties of composite structural insulated panels, Arch. Acoust. 39 (3) (2014) 351–364.
[25] P. Santos, L. Sousa, L. Godinho, J.R. Correia, A. Dias, Acoustic and thermal behaviour of cross-insulated timber panels, J. Build. Eng. (2021) 103309.
[26] ISO 10140-2, Acoustics - Laboratory measurement of sound insulation of building elements - Part 2: Measurement of airborne sound insulation, International Organization for Standardization, Genève, 2010.
[27] ISO 10140-3, Acoustics - Laboratory measurement of sound insulation of building elements - Part 3: Measurement of impact sound insulation, International Organization for Standardization, Genève, 2010.
[28] B. Sharp, Prediction methods for the sound transmission of building elements, Noise Control Eng. 11 (1978).
[29] I. Bosmans, P. Mees, G. Vermeir, Structure-borne sound transmission between thin orthotropic plates: analytical solutions, J. Sound Vib. 191 (1) (1996) 75–90, https://doi.org/10.1006/jsvi.1996.0107.
[30] ISO 10140-4, Acoustics - Laboratory measurement of sound insulation of building elements - Part 4: Measurement procedures and requirements, International Organization for Standardization, Genève, 2010.
[31] ISO 140-4, Acoustics - Measurement of sound insulation in buildings and of building elements — Part 4: Field measurements of airborne sound insulation between rooms, International Organization for Standardization, Genève, 1998.
[32] EN 12354-1, Building acoustics. Estimation of acoustic performance in buildings from the performance of elements. Airborne sound insulation between rooms, European Committee for Standardization, Brussels, 2000.
[33] ISO 354. Acoustics — Measurement of sound absorption in a reverberation room. International Organization for Standardization, Genève, 2003.
[34] ISO 10140–5. Acoustics — Laboratory measurement of sound insulation of building elements — Part 5: Requirements for test facilities and equipment. International Organization for Standardization, Genève, 2021.
[35] L. Godinho, R. Masgalos, A. Pereira, F.G. Branco, On the use of a small-sized acoustic chamber for the analysis of impact sound reduction by floor coverings, Noise Control Eng. J. 58 (6) (2010) 658–668.
[36] MATLAB, 9.7.0.1190202 (R2019b), The MathWorks Inc., Natick, Massachusetts, 2018.
[37] EN ISO 12354–2. Building acoustics – Estimation of acoustic performance of building from the performance of elements – Part 2: Impact sound insulation between rooms, European Committee for Standardization (CEN), Brussels, Belgium, 2000.
[38] A. Neves e Sousa Experimental and numerical analysis of the acoustic behaviour of GFRP and GFRP-ECC hybrid sandwich panels, Task 8 Report, FCT Project REHABGFRP - Rehabilitation of Building Floors with Lightweight High Performance GFRP Sandwich Panels (PTDC/ECM/113041/2009), 2009.
[39] ISO 717–1. Acoustics - Rating of sound insulation in buildings and of building elements - Part 1: Airborne sound insulation. International Organization for Standardization, Genève, 2013.
[40] A. Neves e Sousa, B. Gibbs, Low frequency impact sound transmission in dwellings through homogeneous concrete floors and floating floors, Appl. Acoust. 72 (4) (2011) 177–189.
[41] ISO 717–2. Acoustics - Rating of sound insulation in buildings and of building elements - Part 2: Impact sound insulation. International Organization for Standardization, Genève, 2013.
[42] M. Heckl, E.J. Rathe, Relationship between the transmission loss and the impact-noise isolation of floor structures, J. Acoust. Soc. Am. 35 (11) (1963) 1825–1830, 1963.
[43] K. Nering, A. Kowalska-Koczwara, Determination of vibroacoustic parameters of polyurethane mats for residential building purposes, Polymers 14 (2022) 314, https://doi.org/10.3390/polym14020314.
[44] M. Ridha, Mechanical and Failure Properties of Rigid Polyurethane Foam under Tension, PhD thesis. National University of Singapore, 2007.
[45] W. Witkiewicz, A. Zieliński, Properties of the polyurethane (PU) light foams, Adv. Mater. Sci. 6 (2) (2006) 35–51.
[46] H. Chung, G. Emms, K. McGunnigle, G. Dodd. Improving the impact insulation of light timber floors'. In *First Australasian Acoustical Societies Conference, Noise of Progress, Proceedings of 1st Joint Australasian Acoustical Conference*, *Christchurch, New Zealand*, 2006.
[47] Portuguese Republic. Portaria n.º 305/2019, Diário da República n.º 175/2019, Série I de 2019–09-12, 2019 (in Portuguese).
[48] Portuguese Republic. Regulation for the Acoustic Requirements of Buildings (Decreto-Lei n.º 96/2008), Diário da República n.º 110/2008, Lisbon, 2008 (in Portuguese).
[49] M.F.F. Neto, S.R. Bertoli, Critérios de desempenho acústico em edifícios residenciais, Acústica e Vibrações nº 43 (2011) 19–29.
[50] B. Rasmussen, T. Carrascal García, Acoustic regulations for offices-Comparison between selected countries in Europe, *INTER-NOISE NOISE-CON Congr. Conf. Proc.* 259 (1)) (2019) 8141–8150.
[51] J.R. Correia, M. Proença, M. Garrido, A. Neves e Sousa, M.G. Gomes, J. Sena-Cruz. Easy Floor Project (ANI 3480/2015). Final Project Report. CERIS. ISSN: 0871-7869.
[52] M. Proença, M. Garrido, J.R. Correia, J. Sena-Cruz, Experimental study on the fire resistance of all-composite and hybrid web-core sandwich panels for building floors, Compos. Struct. 337 (2024) 118071.